

Three-dimensional Permeability Inversion Using Convolutional Neural Networks for Better Prediction of Contaminant Transport in Aquifer Materials



Zitong Huang (zhuang296@wisc.edu) and Christopher Zahasky (czahasky@wisc.edu)

Department of Geoscience

Introduction

Recent utilization of medical imaging techniques in hydrogeology allows the measurement of solute concentrations in spatial and temporal dimensions. Establishing the relationship between concentration distributions and permeability fields will improve modeling of contaminant transport in complex geologically systems. This study presents an inversion method utilizing a regressive neural network that can efficiently approximate the 3D permeability field of geologic samples using imaging-derived concentration measurements.

Data

We used 50% quantile concentration arrival time in each voxel to reduce the dimensionality of the imaging data. An example of the imaging experimental data is shown in Figure 1 and 2. 20,000 synthetically generated permeability fields are used for training, validation, and test data for the CNN. A traditional numerical modeling approach was used to produce the arrival time maps.

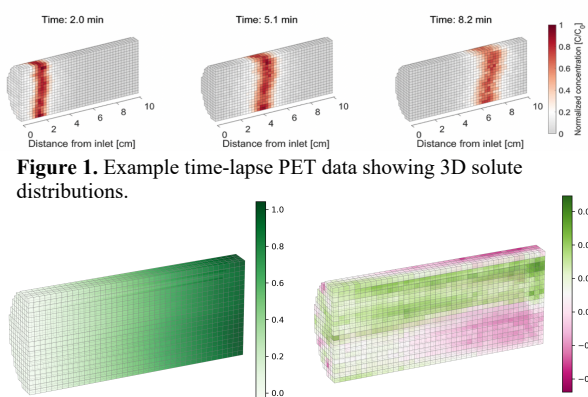


Figure 1. Example time-lapse PET data showing 3D solute distributions.
Figure 2. (left) Normalized arrival time map of PET data in Figure 1 and corresponding normalized arrival time difference map (right).

Methods

- The inverse modeling problem (i.e. arrival time to permeability field) is approached as an image-to-image regression task.
- Each input normalized mean arrival time field has one corresponding labeling permeability fields, so the training process is supervised
- For the input data, the mean permeability ($k = q \cdot \mu \cdot \frac{L}{dP}$) of the sediment column is represented by a column vector at the boundary of injection

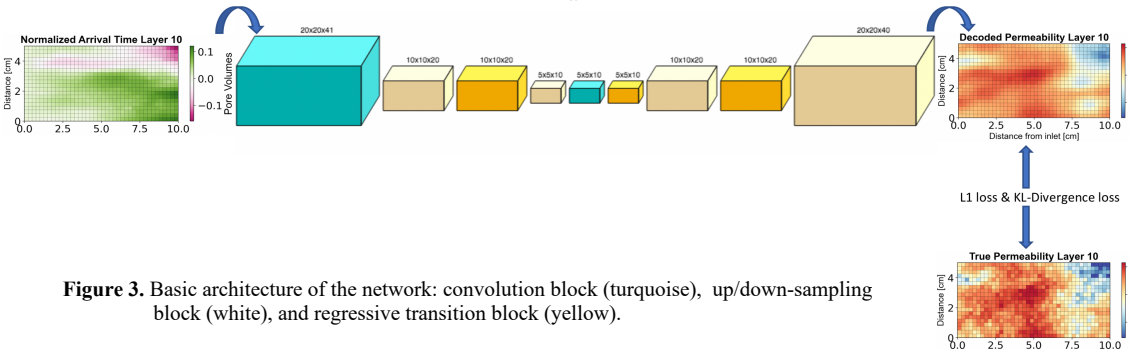
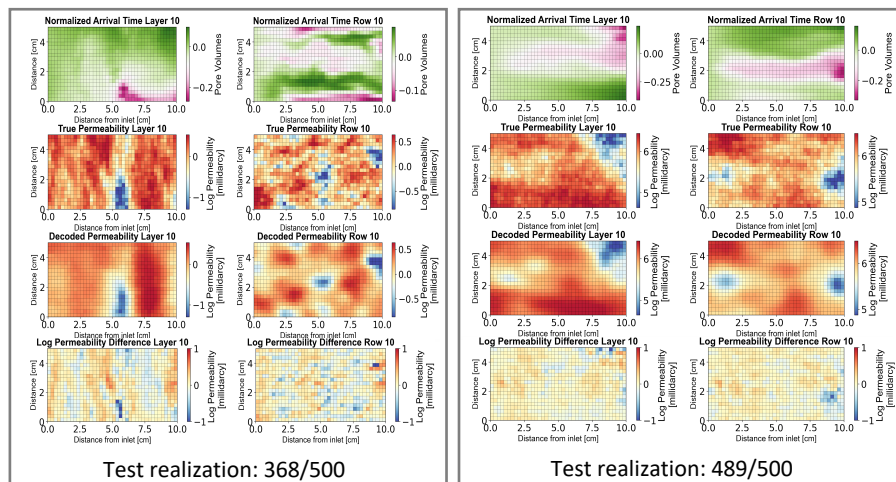
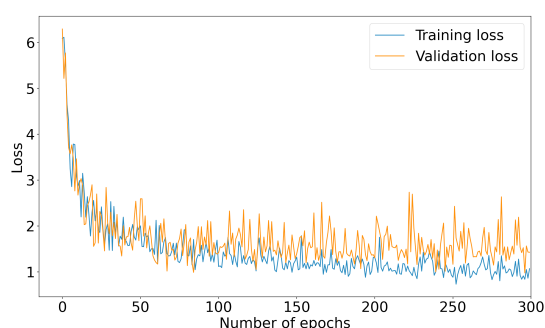


Figure 3. Basic architecture of the network: convolution block (turquoise), up/down-sampling block (white), and regressive transition block (yellow).

Results

Figure 4: Training (blue) and validation (orange) loss function during CNN training. This summarizes the difference between the CNN prediction and the true data.



Figures 5 and 6: Illustration of the input arrival time difference map (top row), the test data permeability fields, and the predicted log permeability fields of 2 testing set examples. The left and right rows correspond to the 2 orthogonal slices through the 3D models.

Summary

- The network can predict the general pattern of the permeability fields and mean value.
- When the permeability field is very homogeneous (having a very narrow range of values), the network fails to capture very subtle patterns.
- Future work will focus on quantifying network efficacy with statistical analysis of the test set (the data not used for training and validation), loss propagating strategies, and how to incorporate additional physics-based constraints.

References

- He, K., Zhang, X., Ren, S., & Sun, J. (2016a). Deep residual learning for image recognition. In *IEEE Conference on Computer Vision and Pattern Recognition (CVPR)*.
- Huang, G., Liu, Z., Van Der Maaten, L., & Weinberger, K. Q. (2017). Densely connected convolutional networks. In *IEEE Conference on Computer Vision and Pattern Recognition (CVPR)*, pp. 2261–2269.
- Mo, S., Zabaras, N. J., Shi, X., & Wu, J. (2020). Integration of adversarial autoencoders with residual dense convolutional networks for estimation of non-Gaussian hydraulic conductivities. *Water Resources Research*, 56, e2019WR026082.